

A Comparison of Approaches for Modelling an 8P Ultrasonic Flowmeter

Patrick Arnould – Robert Gordon University. Email: p.arnould@rgu.ac.uk

Supervisor: Prof. Mamdud Hossain

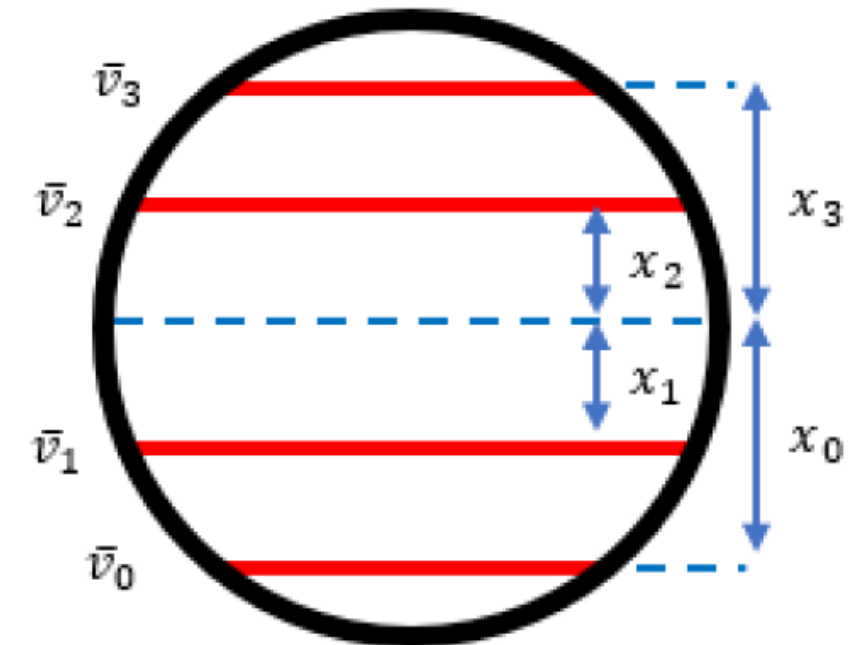
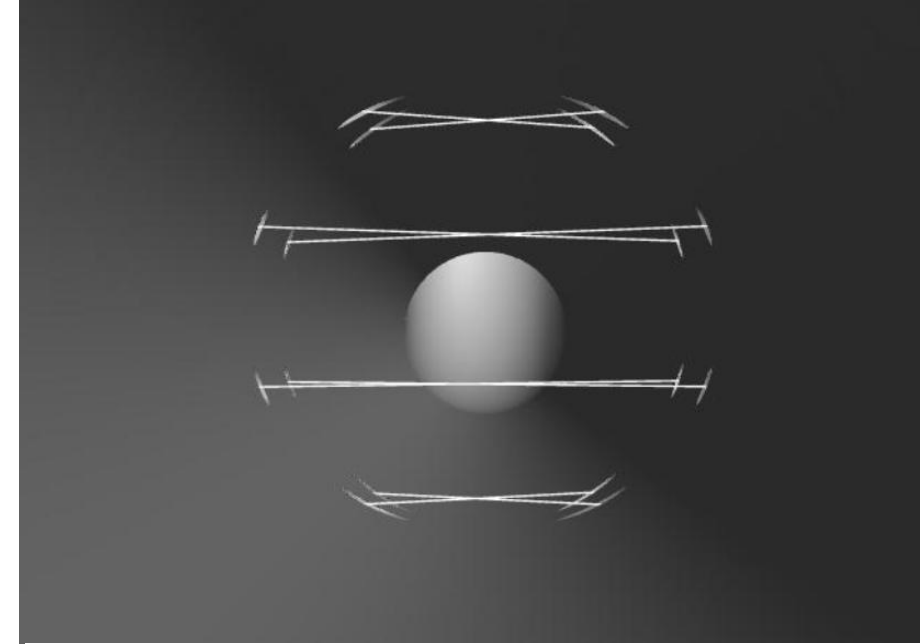
Industrial Advisor: Dr. Gregor Brown

Agenda

- Introduction
- Analytical and Experimental Results
- Reducer & Cavity Effects on Meter Factor in Straight Pipe
- Acoustic Model Overview & Validation
- Acoustic Model Results vs Experiment
- Modelling Triple Bend
- Summary

Introduction

- My research considers existing and new methods to design and evaluate **integration schemes** for **chordal** ultrasonic flowmeters
- Various new and existing designs evaluated using an analytical model. UFM with correct path positions available which also permitted comparison of two designs in flow laboratory
- This presentation summarises the analytical and experimental results and subsequent investigation

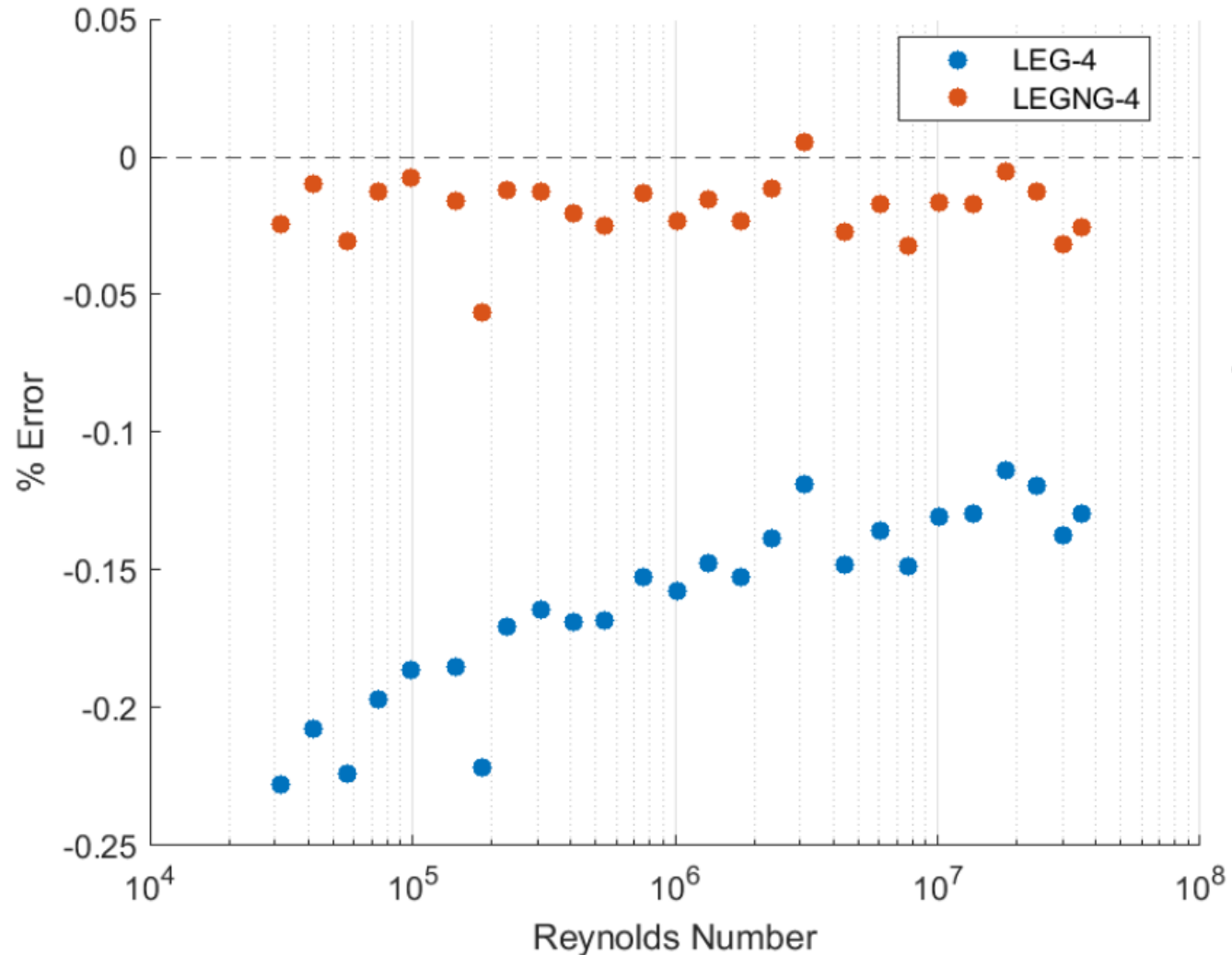


$$\bar{V} \approx \sum_{k=0}^n f(x_k) \int_{-1}^1 \ell_k(x) w(x) dx = \sum_{k=0}^n f(x_k) w_k$$

Integration Schemes Compared

	Gauss-Legendre LEG-4	Revised Legendre LEGNG-4
Chord Positions $x_k (x_3 = -x_0, x_2 = -x_1)$	$x_0 = -0.861136$ $x_1 = -0.339981$	
Weighting factors $w_k (w_3 = w_0, w_2 = w_1)$	$w_0 = 0.111905$ $w_1 = 0.388095$	$w_0 = 0.107364$ $w_1 = 0.392636$

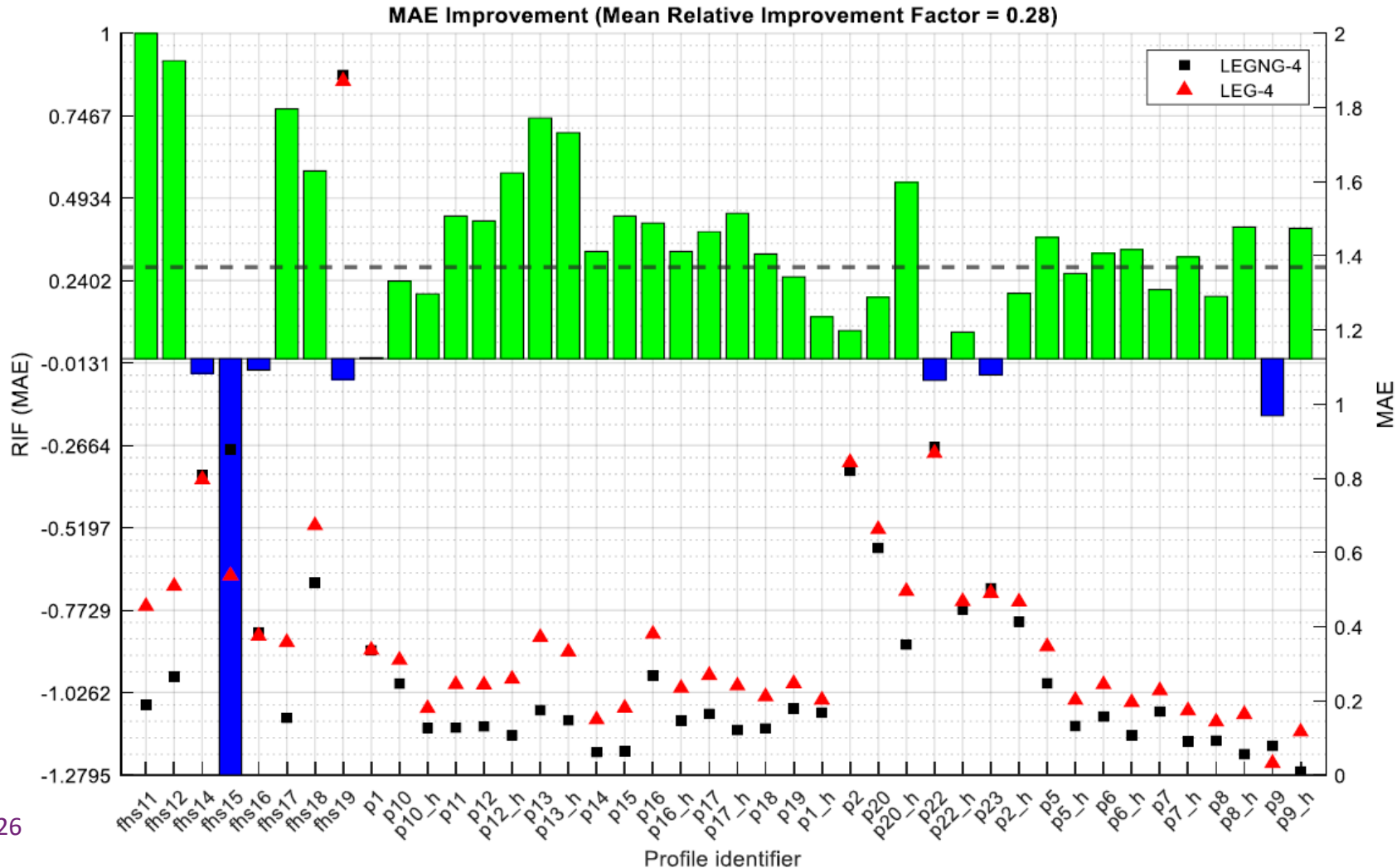
Analytical Results – Straight Pipe



**Note this is showing % error.
LEG-4 Meter factor
(Q_{ref}/Q_{mut}) would be > 1 and
decreasing as Reynolds
number increases**

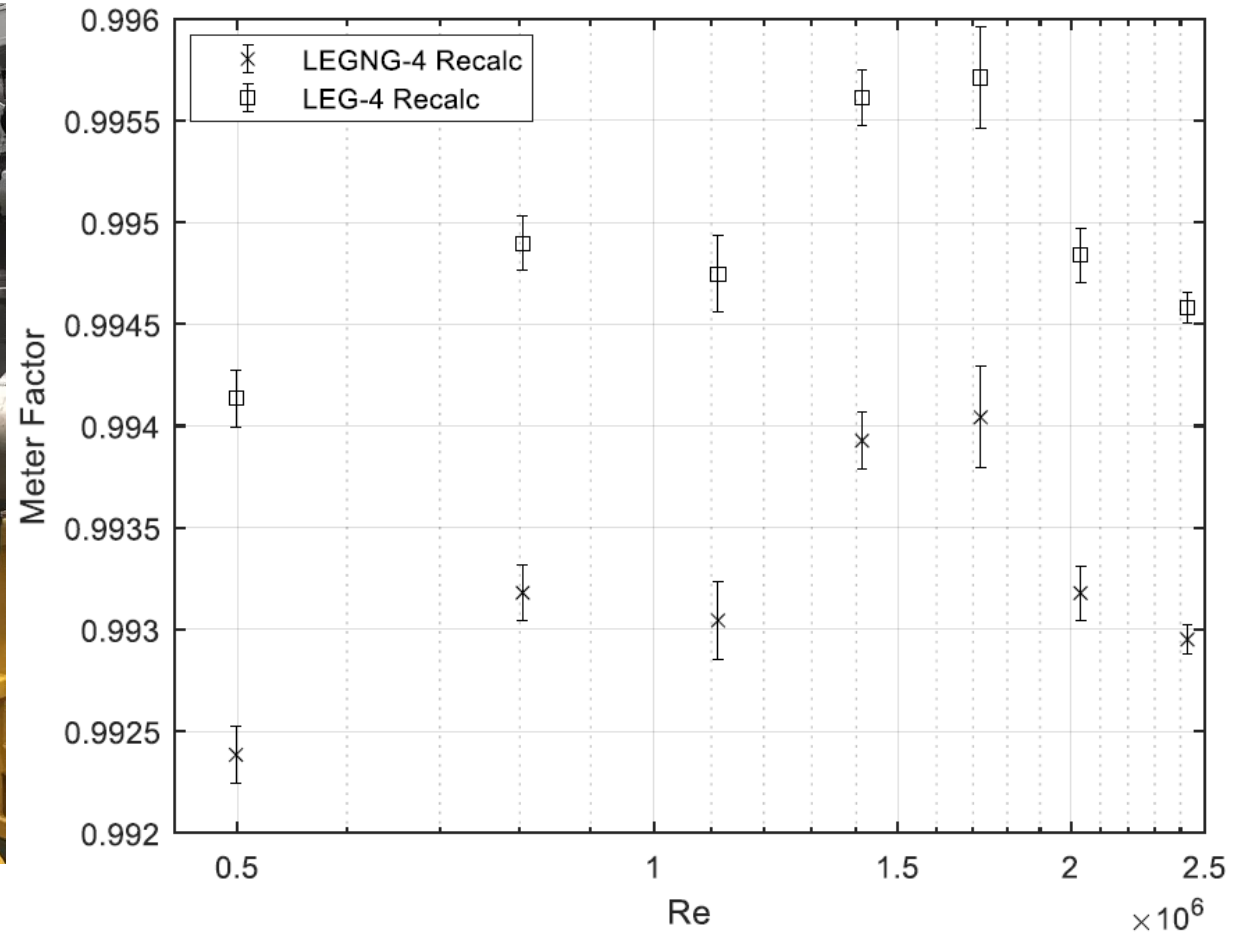
**LEGNG shows clear
improvement**

Analytical Results – Disturbed Profiles

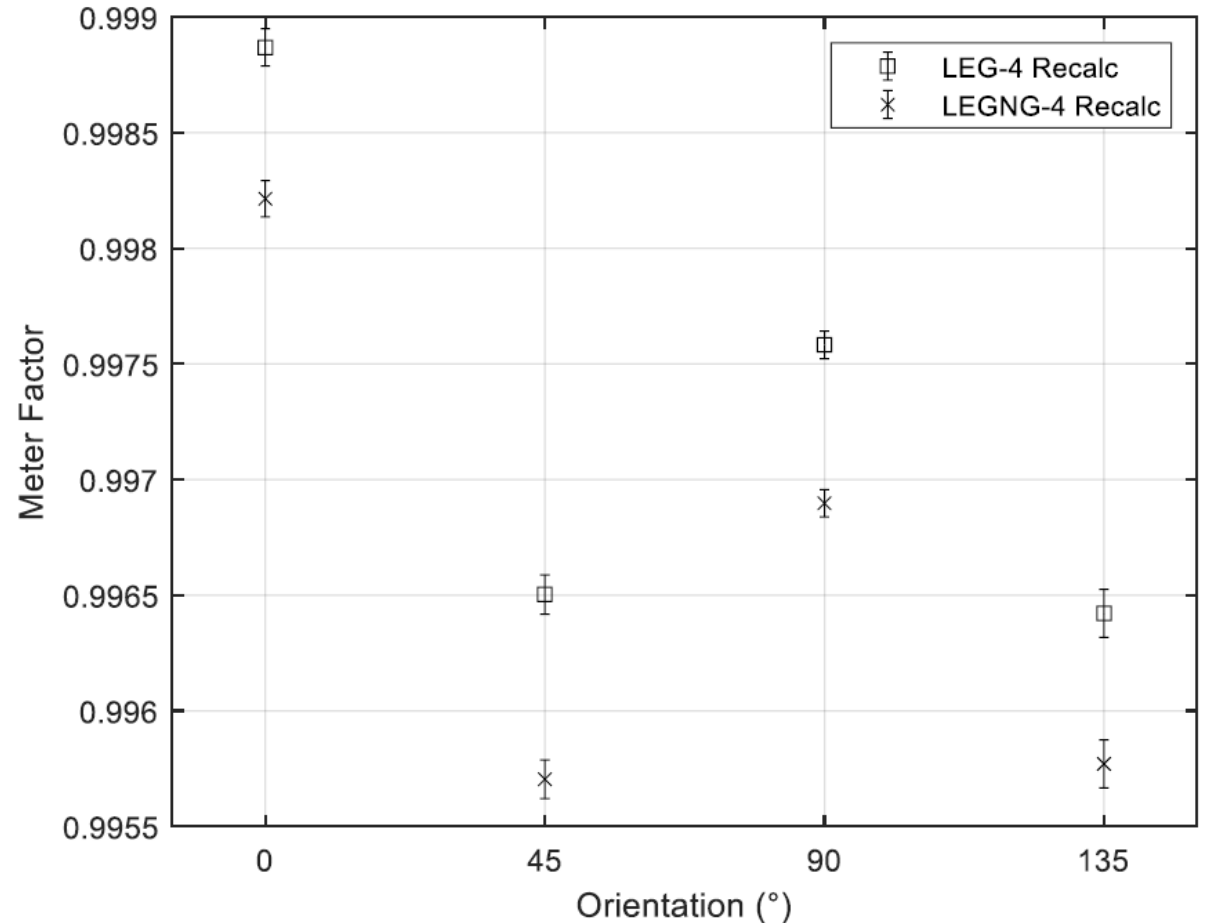


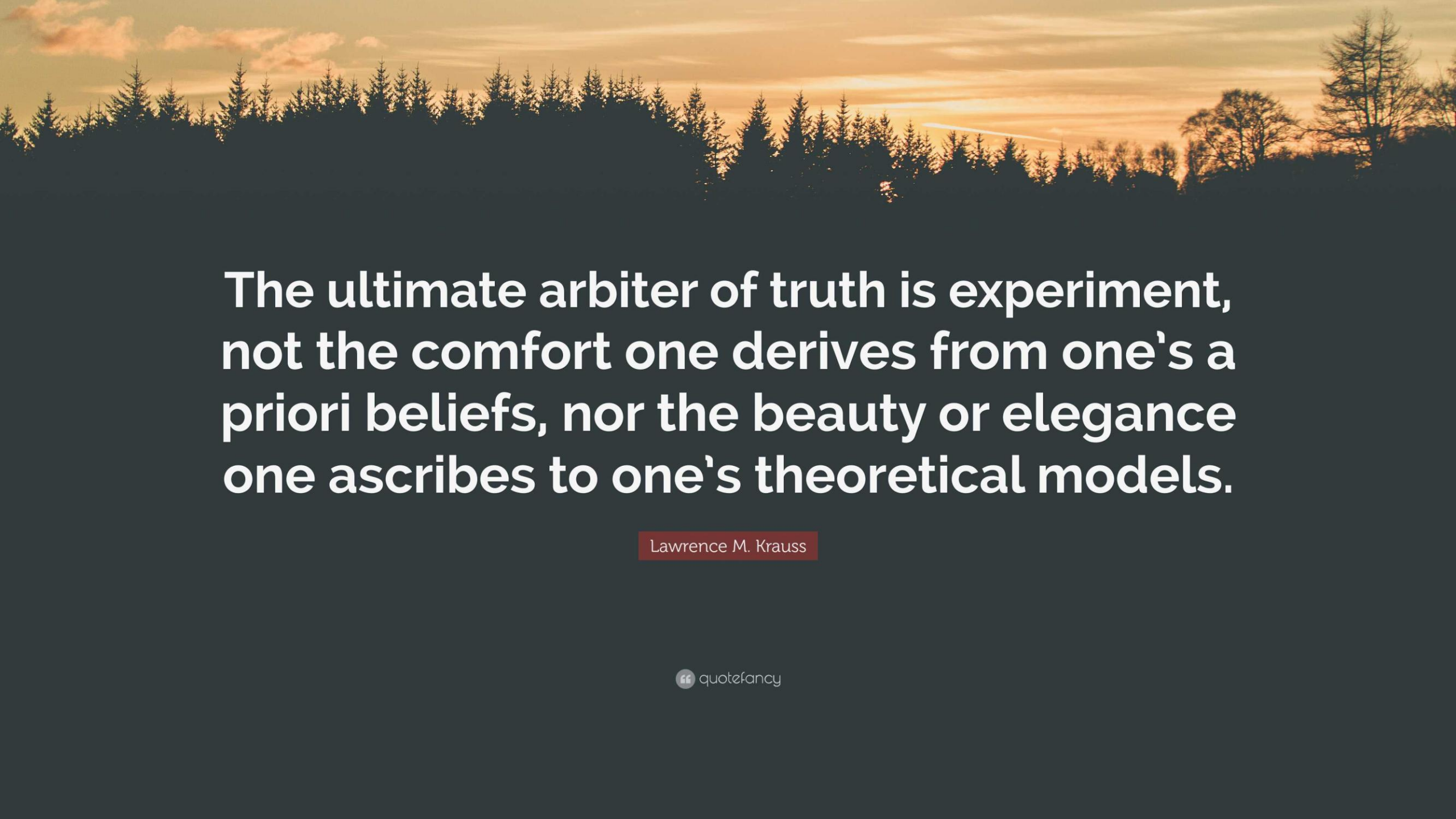
LEGNG again shows clear improvement

Experimental Results – Straight Pipe (Raw)



Experimental Results – Triple Bend 10D (Raw)

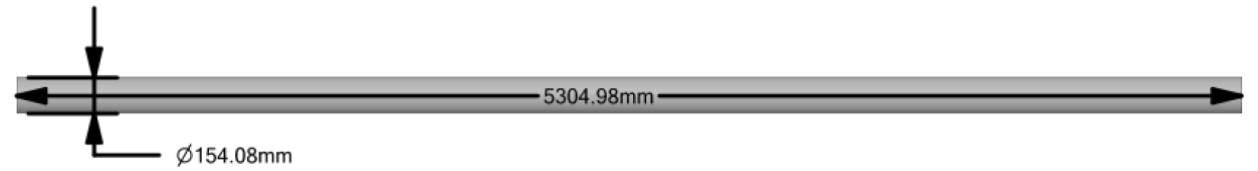


A sunset over a forest of evergreen trees. The sky is a mix of orange, yellow, and light blue, with a few wispy clouds. The trees are silhouetted against the bright sky. A thin white line, possibly a contrail, is visible in the sky.

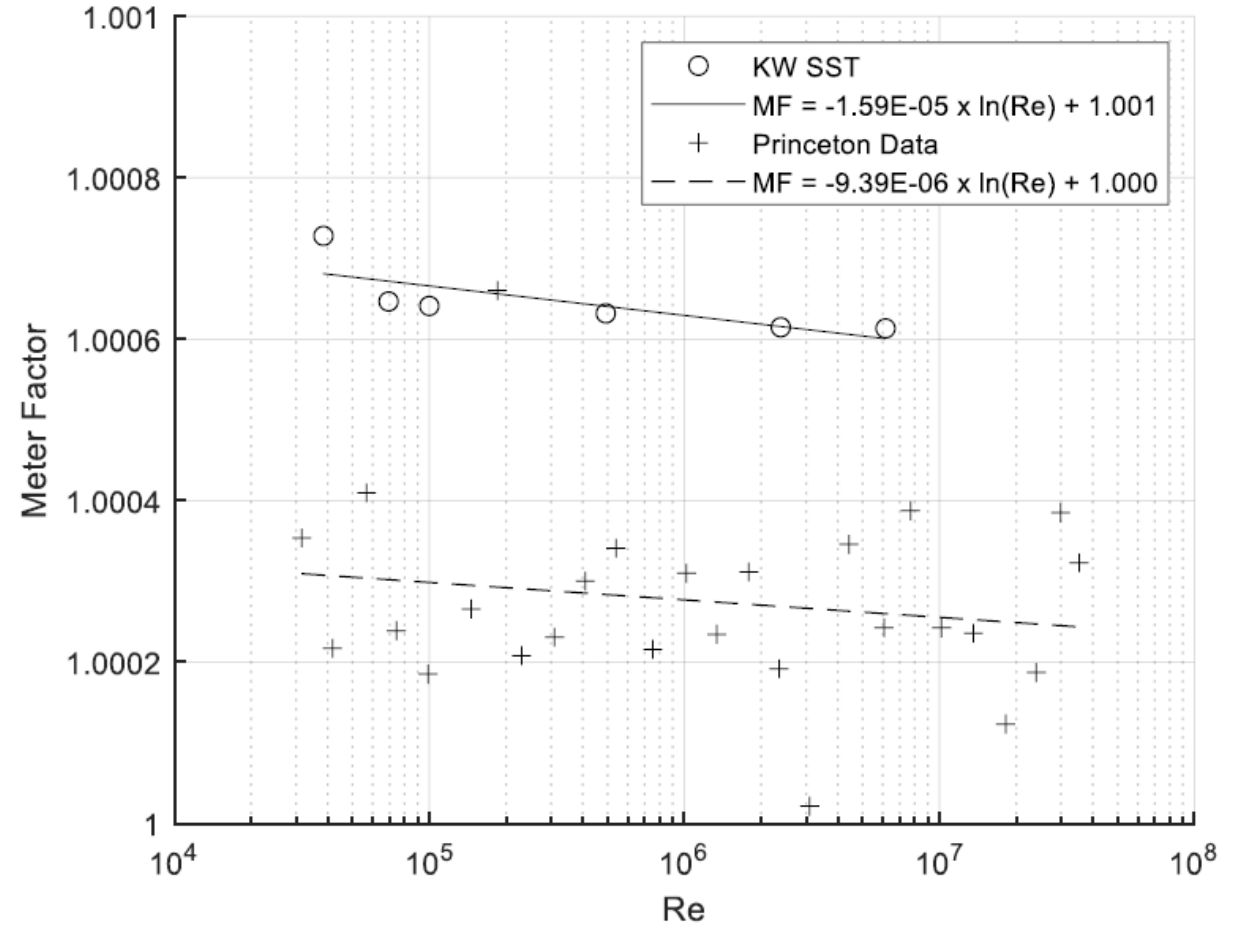
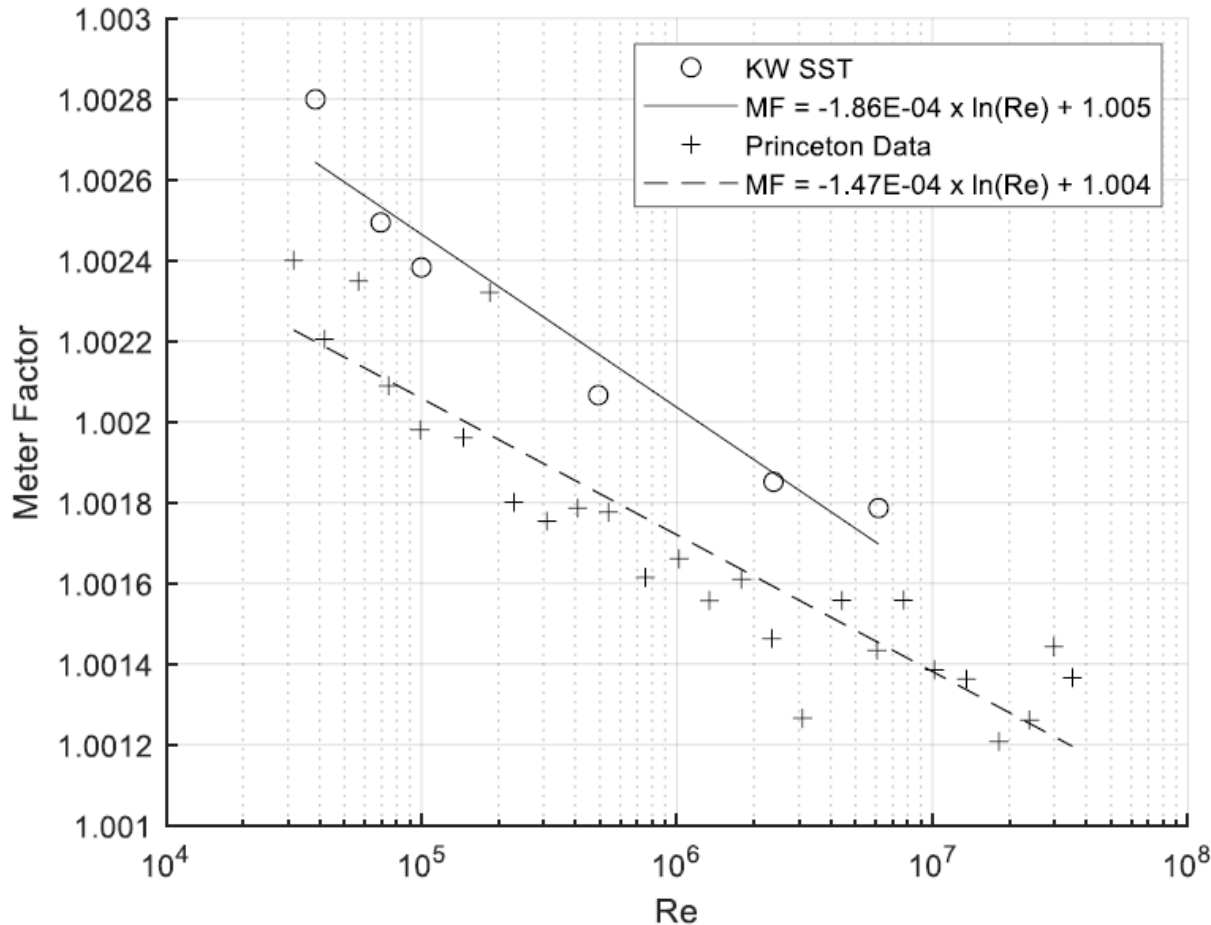
**The ultimate arbiter of truth is experiment,
not the comfort one derives from one's a
priori beliefs, nor the beauty or elegance
one ascribes to one's theoretical models.**

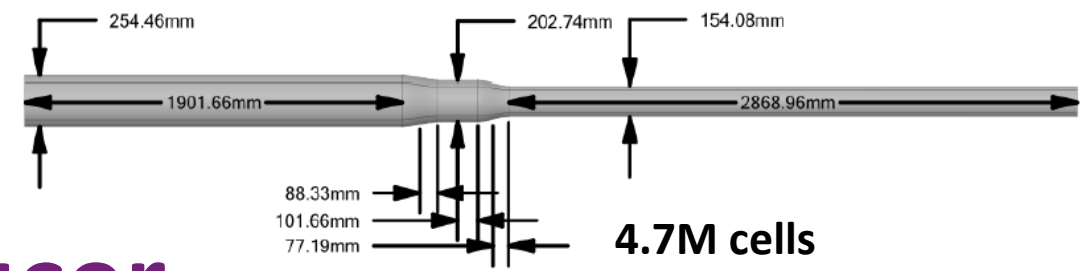
Lawrence M. Krauss

4.7M cells

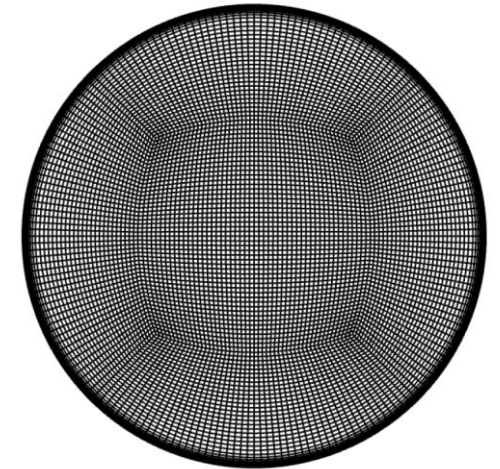
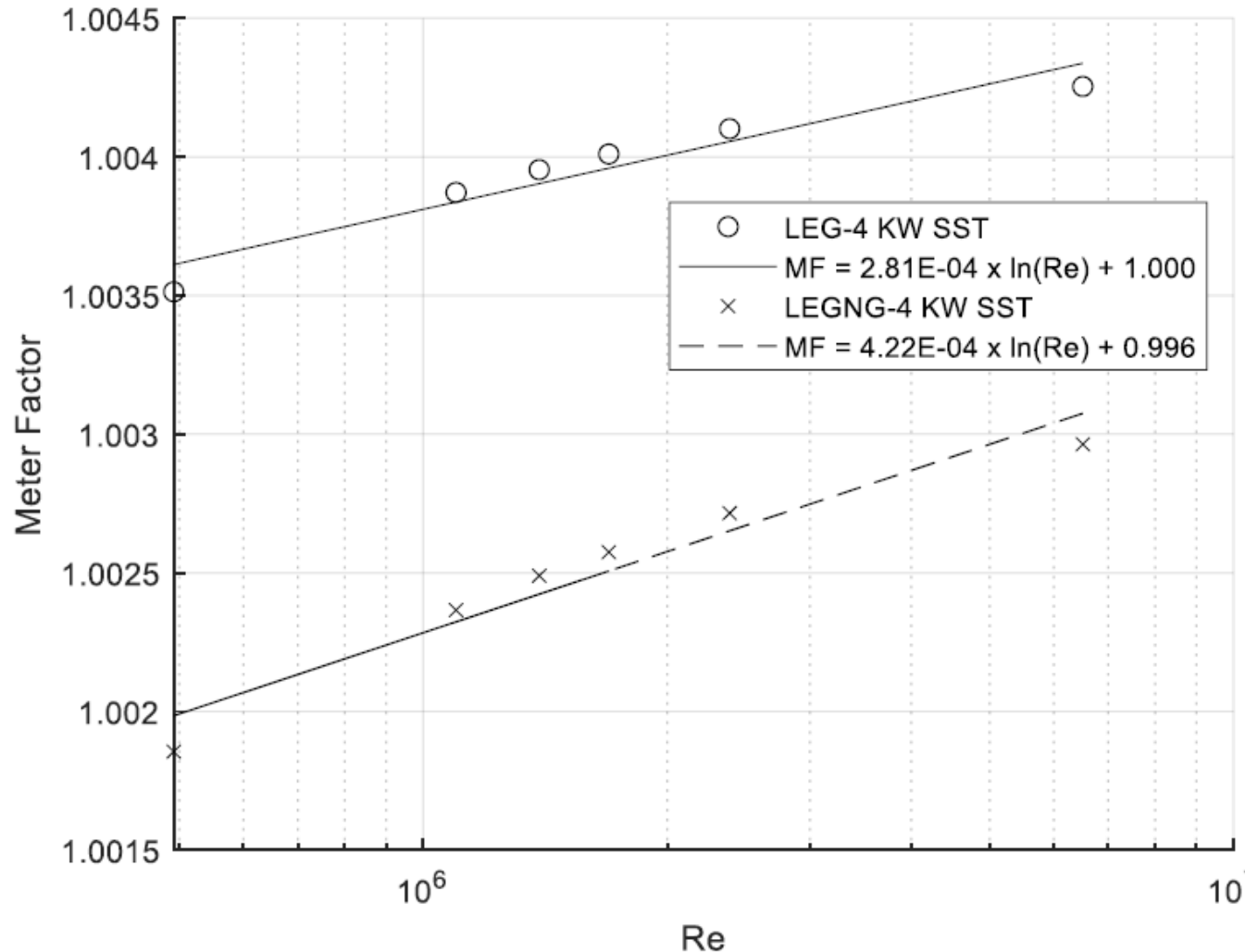


CFD Straight Pipe – Close to Analytical Model



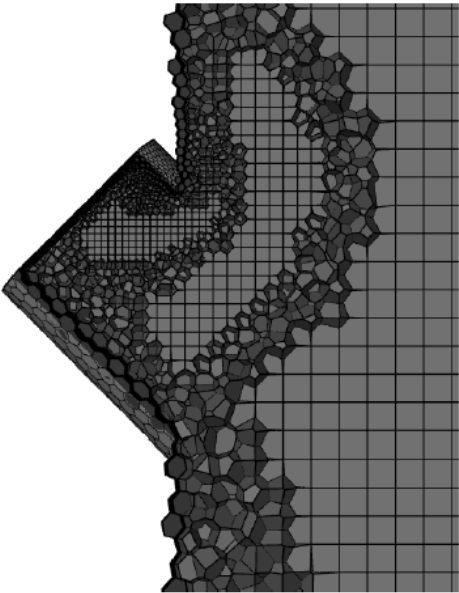
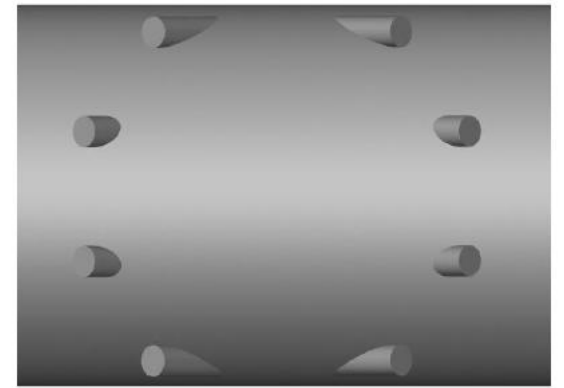


CFD Straight Pipe With Reducer

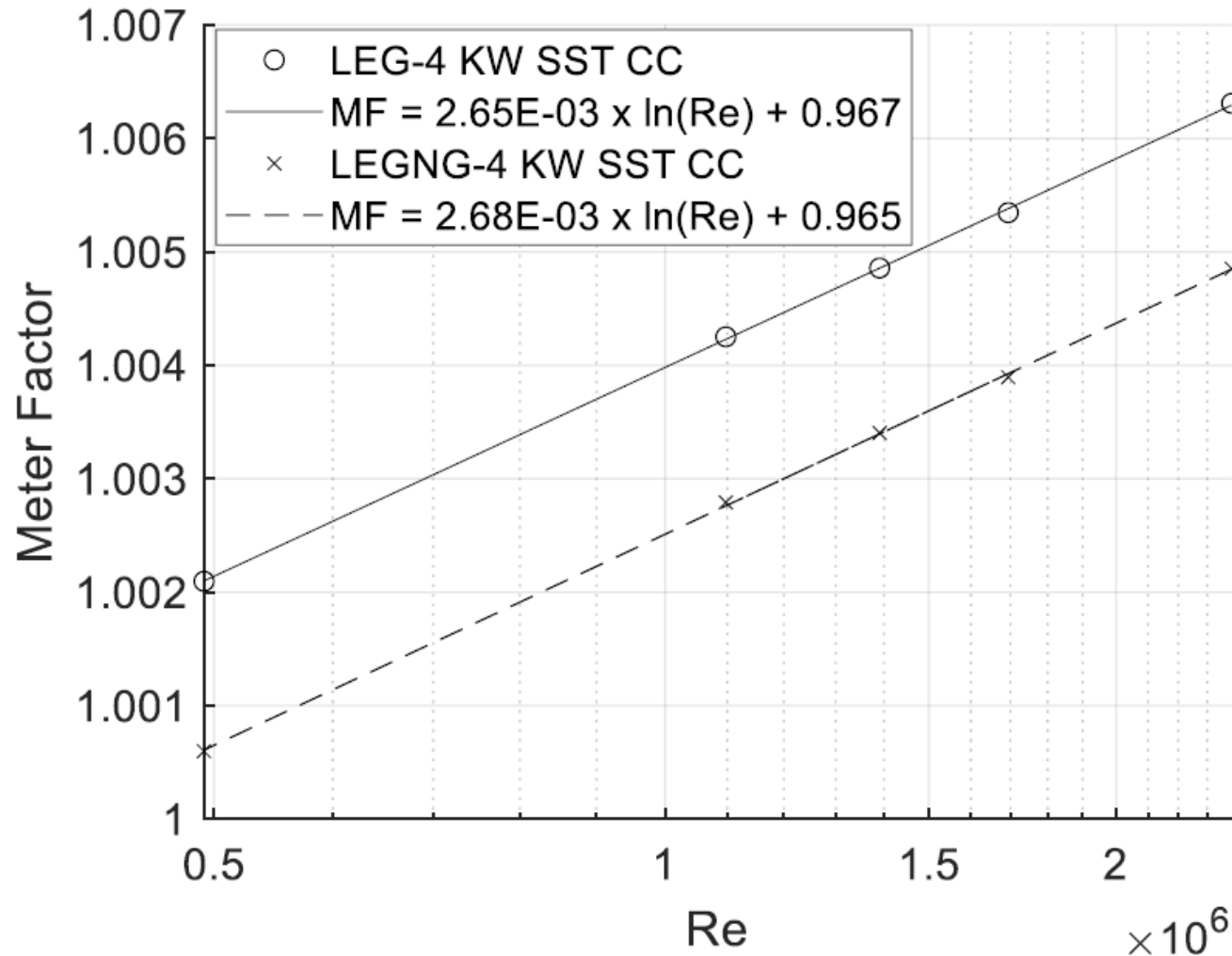


Meter factor now increasing with Reynolds number. LEGNG-4 still closest to 1

CFD Straight Pipe (Reducer, Cavities, Smooth)

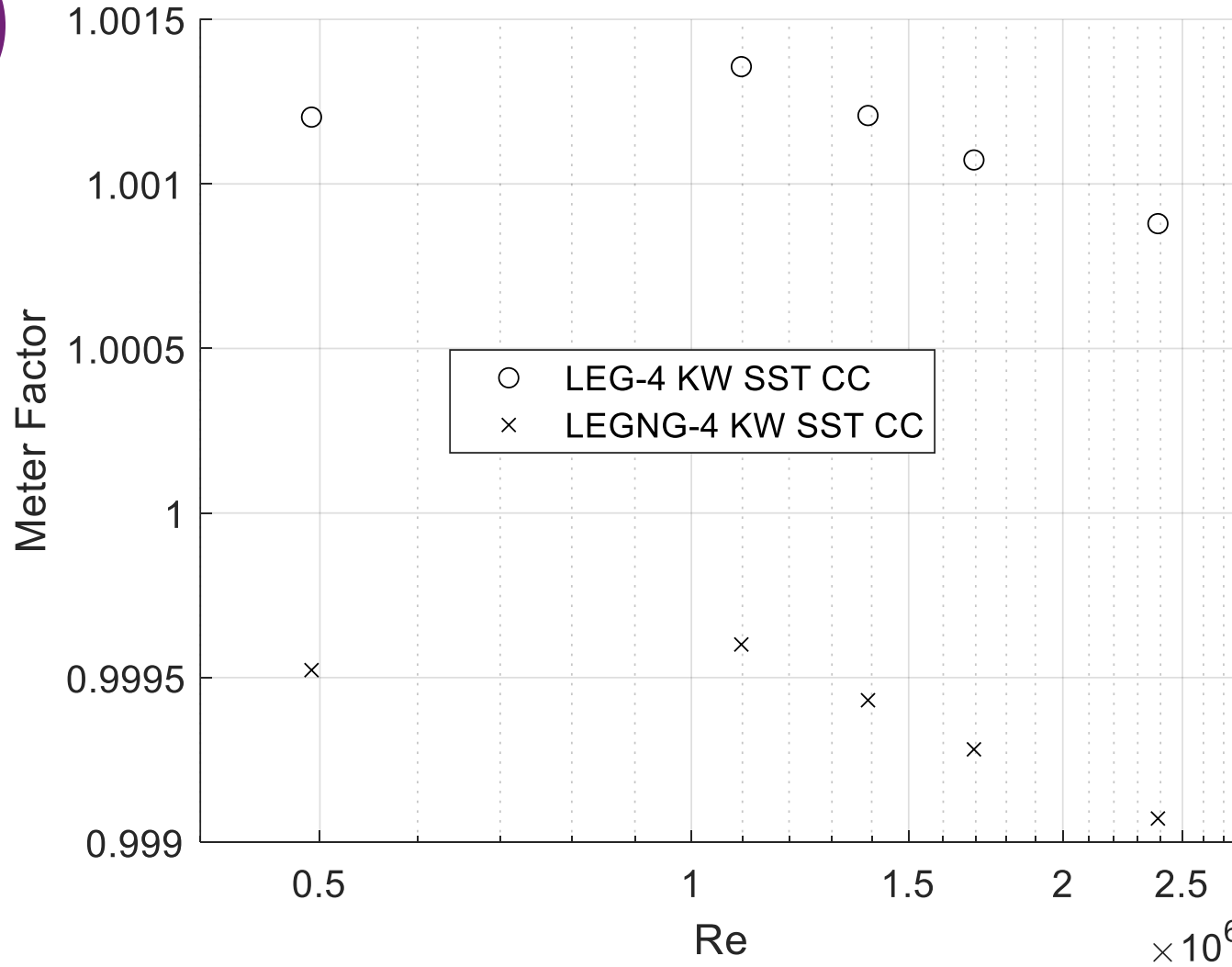
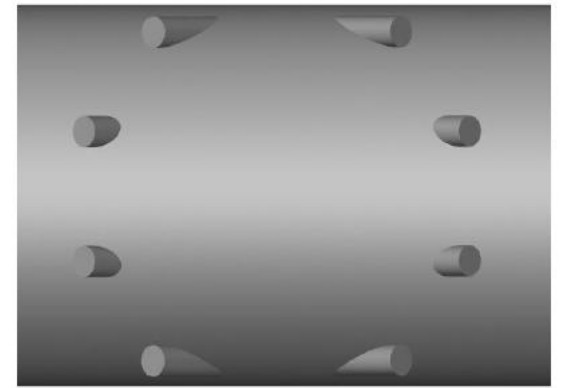


11M cells



**Meter factor reduced,
larger change with
Reynolds number and
LEGNG-4 still closest to 1**

CFD Straight Pipe (Reducer, Cavities, Rough)



Meter factor behaviour closer to experiment but LEGNG-4 still closest to 1. Roughness height 0.09 mm.

Meter factor still far away from that seen during experiment.

Summary of Previous Slides:

Models Still Not Agreeing with Experiment

- Good agreement between CFD and analytical model in straight pipe
- Analytical model ignored effects of reducer, transducer cavities, roughness and assumed developed profile which was not present during experiment
- However, with all those differences accounted for the modelling still incorrectly predicts LEGNG-4 as the best performing integration scheme
- Path velocity has been modelled using single line integral between transducer centres. *What about acoustic effects?*

Acoustic Model Implementation

Time domain Rayleigh integral (classical result) is integrated across receiver area and then discretised

$$p(x, t) = \frac{\rho}{2\pi} \int_{\sigma} \frac{v'(t - R/c)}{R} dS \quad \Rightarrow \quad P_{receiver} = \frac{\rho}{A_R 2\pi} \int_{\varphi} \int_{\sigma} \frac{v'(t - R/c)}{R} dS dA$$

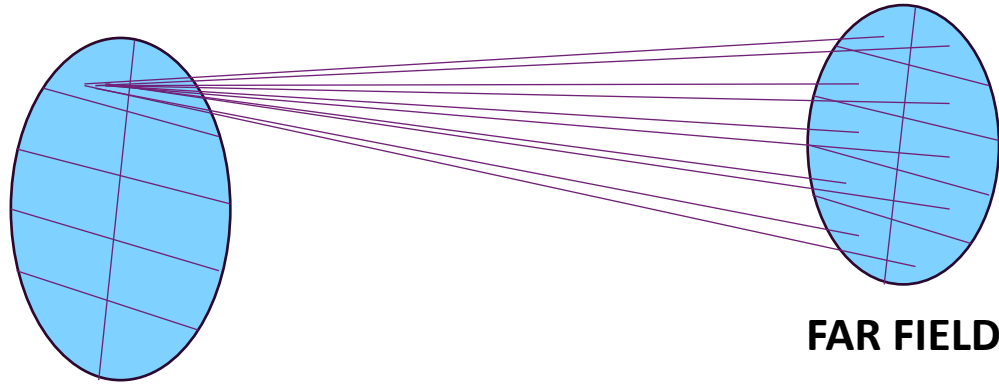
Acoustic pressure at point x and time t

Piston acceleration which occurred R/c seconds before t where R is the distance from the elemental area dS to x , scaled by $1/R$ which represents amplitude correction.

Receiver surface area

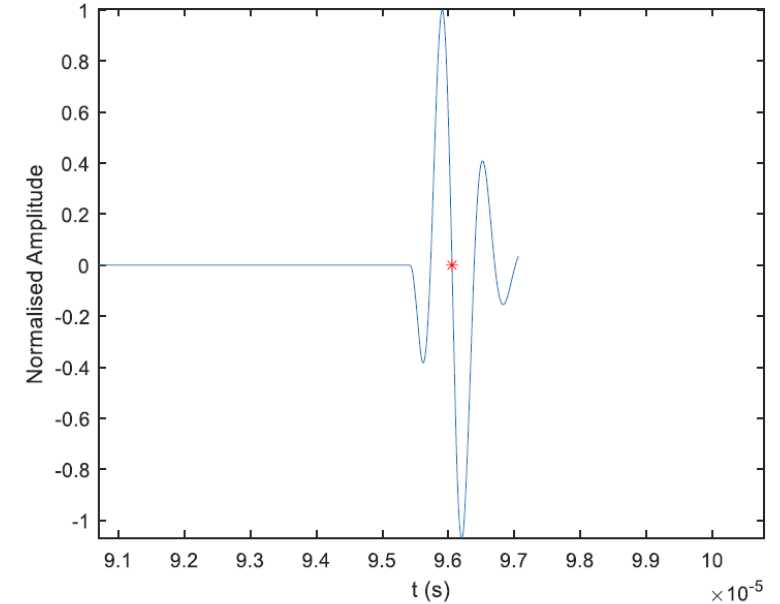
Receiver elemental area

Summary of Acoustic Model



Transit time calculated using line integral and amplitude calculated accounting for acoustic path length and cell areas from single cell on transmitter to **every** cell on the receiver. **Repeat for every cell on transmitter.**

Realistic wavelets scaled by their amplitudes and starting at their respective transit times are then superimposed to produce a composite waveform. Can model piston velocity or acoustic pressure using observed waveforms.



Zero crossing detection algorithm then used on the composite waveform to determine transit time and compute path velocity.

Acoustic Model Validation

- Frequency domain model exists which predicts phase difference between plane wave and composite waveform produced by baffled piston (e.g. Lunde et al. 2025 referencing Khimunin's work)

$$H_{BPDC}^{dif,1}(L, f) = \frac{\langle p^{pist}(L, f) \rangle}{p^{plane}(L, f)} = 1 - \frac{4}{\pi} \int_0^{\pi/2} e^{-i \frac{(kr_t)^2 S_k}{2\pi} \left(\sqrt{1 + \left(\frac{4\pi}{S_k \cdot kr_t} \right)^2 \cos^2 \theta} - 1 \right)} \sin^2 \theta d\theta$$

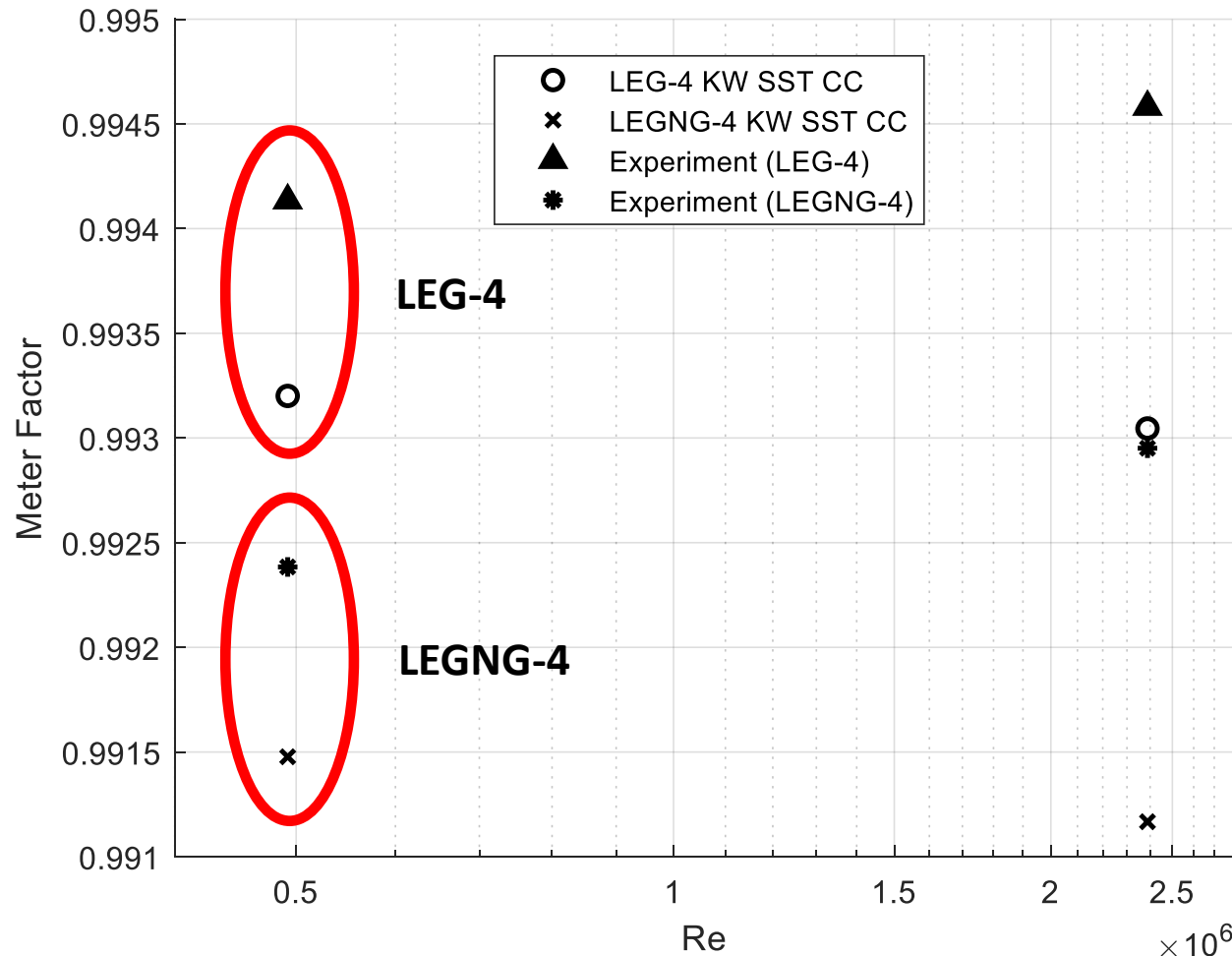
Lunde, P. et al. (2025) Diffraction correction for piezoelectric transducers in precision ultrasonic measurement systems

- The **Discretised Rayleigh Integral** can be compared with this in zero flow using sin wave excitation for single wavelet between transducer centres and full acoustic model (DRI). The FFT of these two responses can be used to compute phase difference between DRI and plane wave.

Acoustic Model Validation

Number of Acoustic Paths	Phase difference between DRI and plane wave (ns)	Phase difference between BPDC and plane wave (ns)	DRI phase difference - BPDC phase difference (ns)
2304	70.71	68.62	2.09
12321	69.53	68.62	0.91
39601	69.16	68.62	0.54

Acoustic Model (Straight, Reducer, Cavities, Rough)



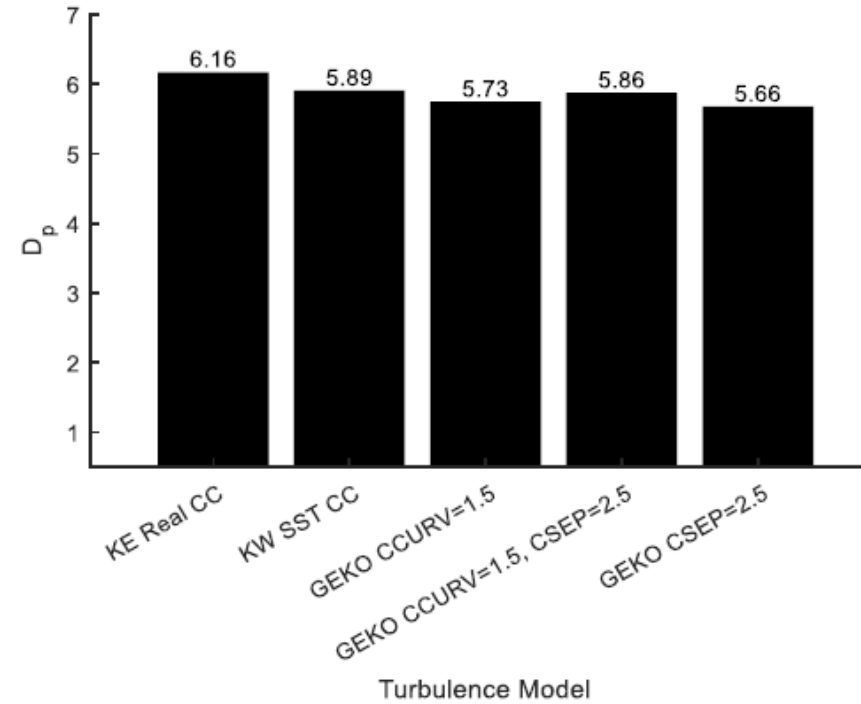
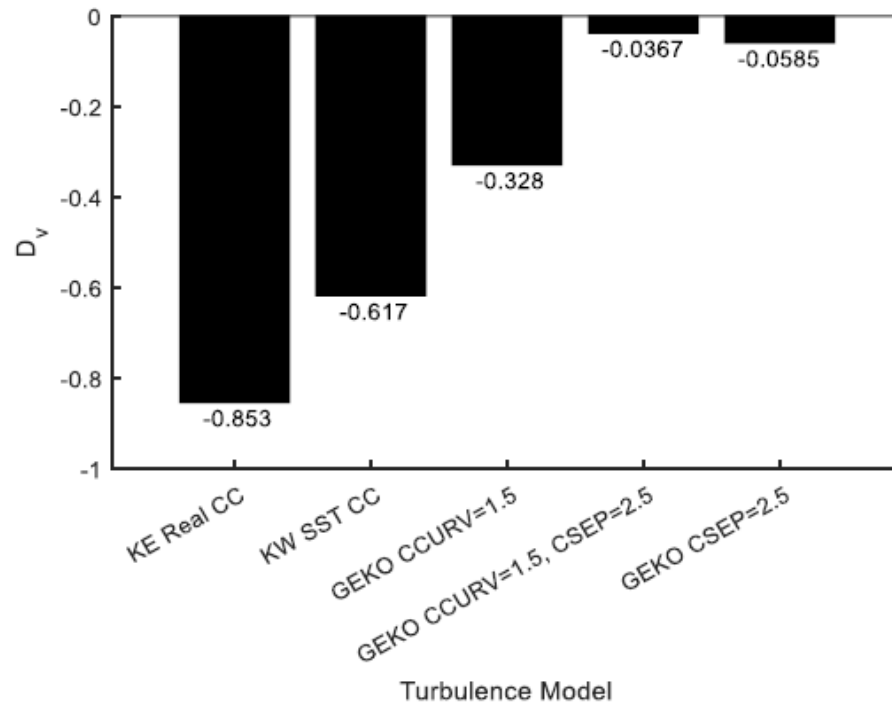
LEG-4 now closest to 1 agreeing with experiment!

Meter factor close to experiment!

Correction resulted in ~0.8% increase in mean velocity when modelling acoustic pressure (~0.6% modelling piston velocity with less realistic wavelet shape)

CFD Triple Bend

- CFD model struggled on this case. % difference between mean velocity during experiment and in CFD misleading, average absolute path velocity difference gave better indication of reality. Acoustic correction didn't help.

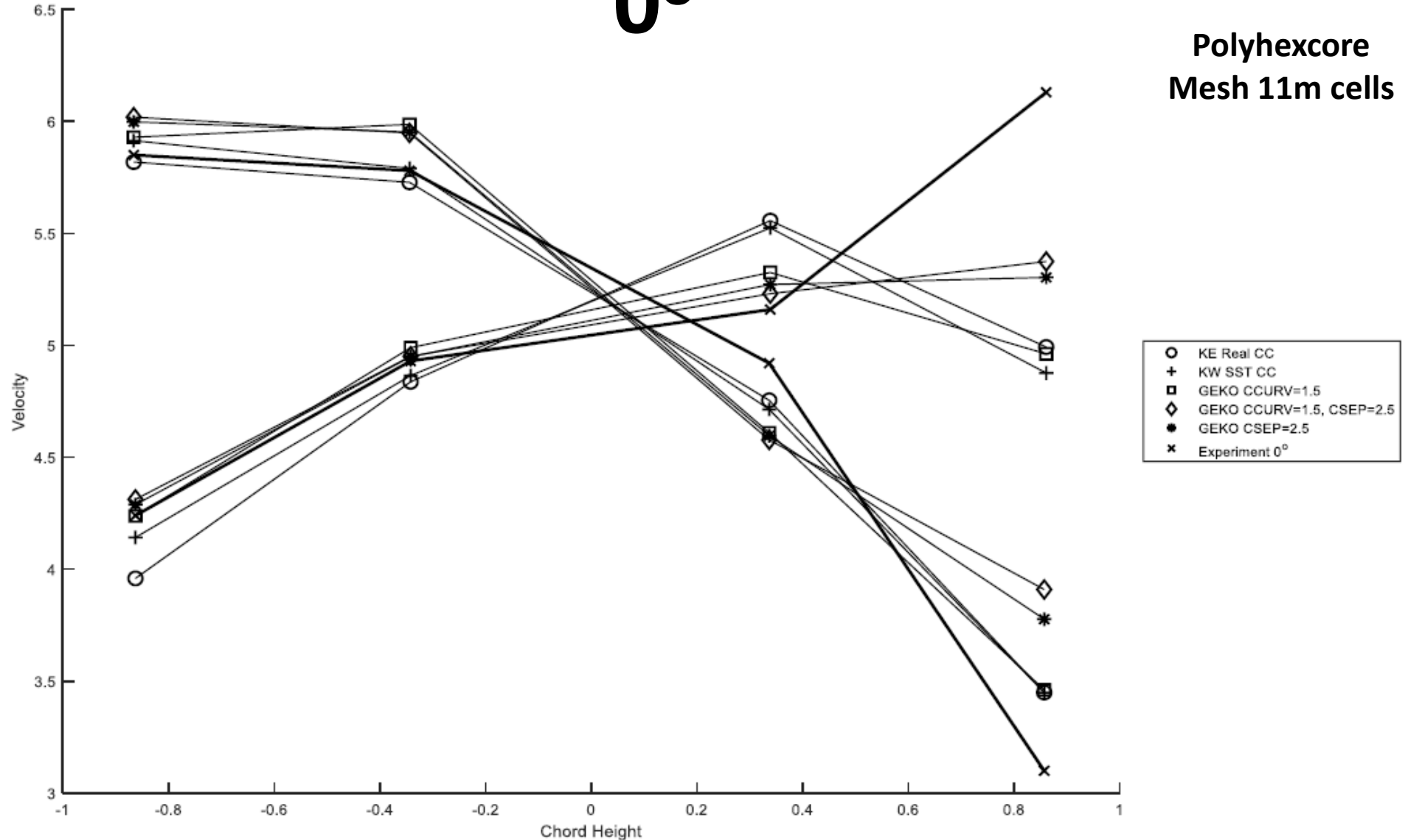


- CFD results appeared to agree better with experimental results at 90° for cavity case and 45° for no cavity case, despite turbulence model tuning

CFD Triple Bend – With Cavities

0°

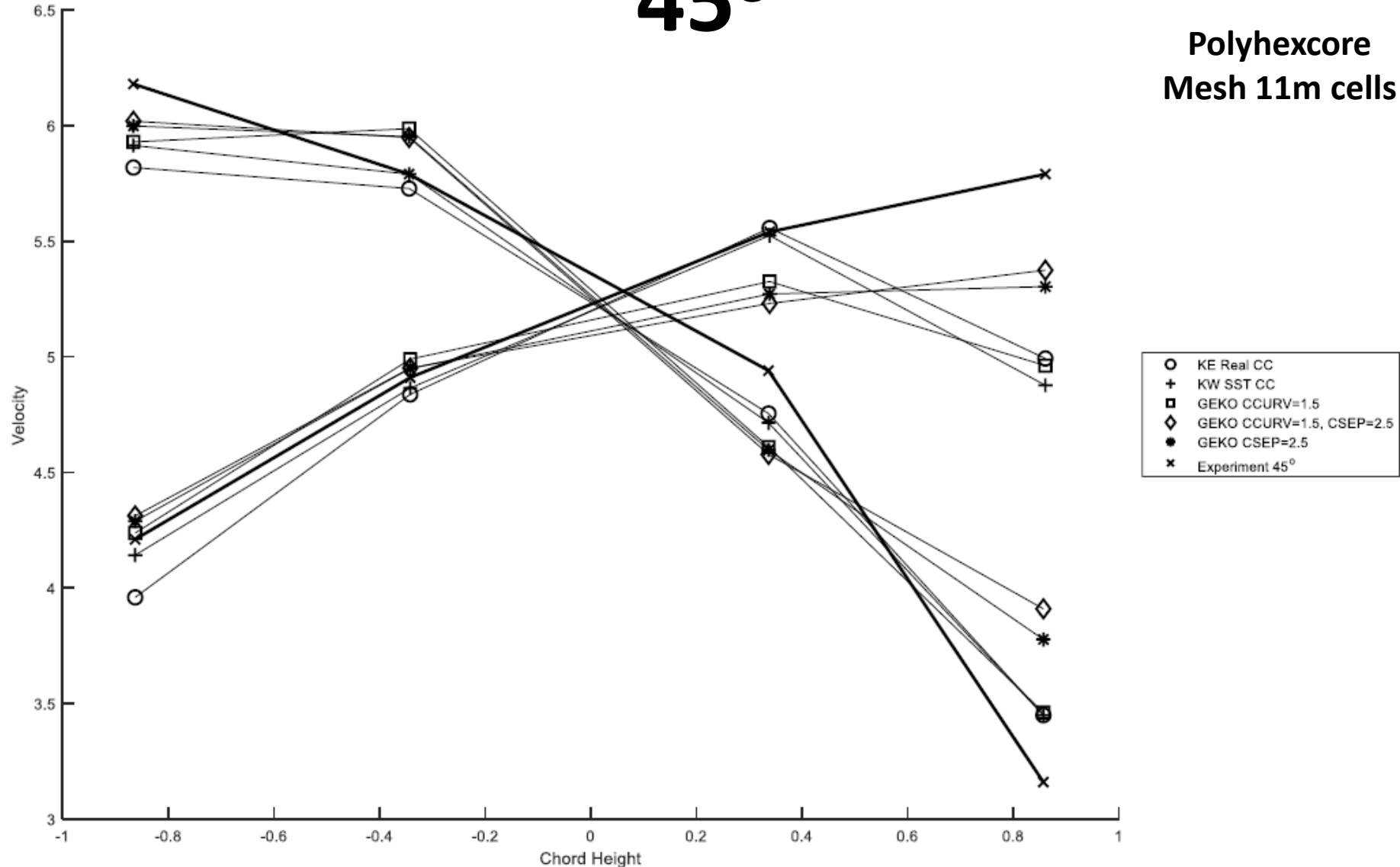
**Polyhexcore
Mesh 11m cells**



CFD Triple Bend – With Cavities

45°

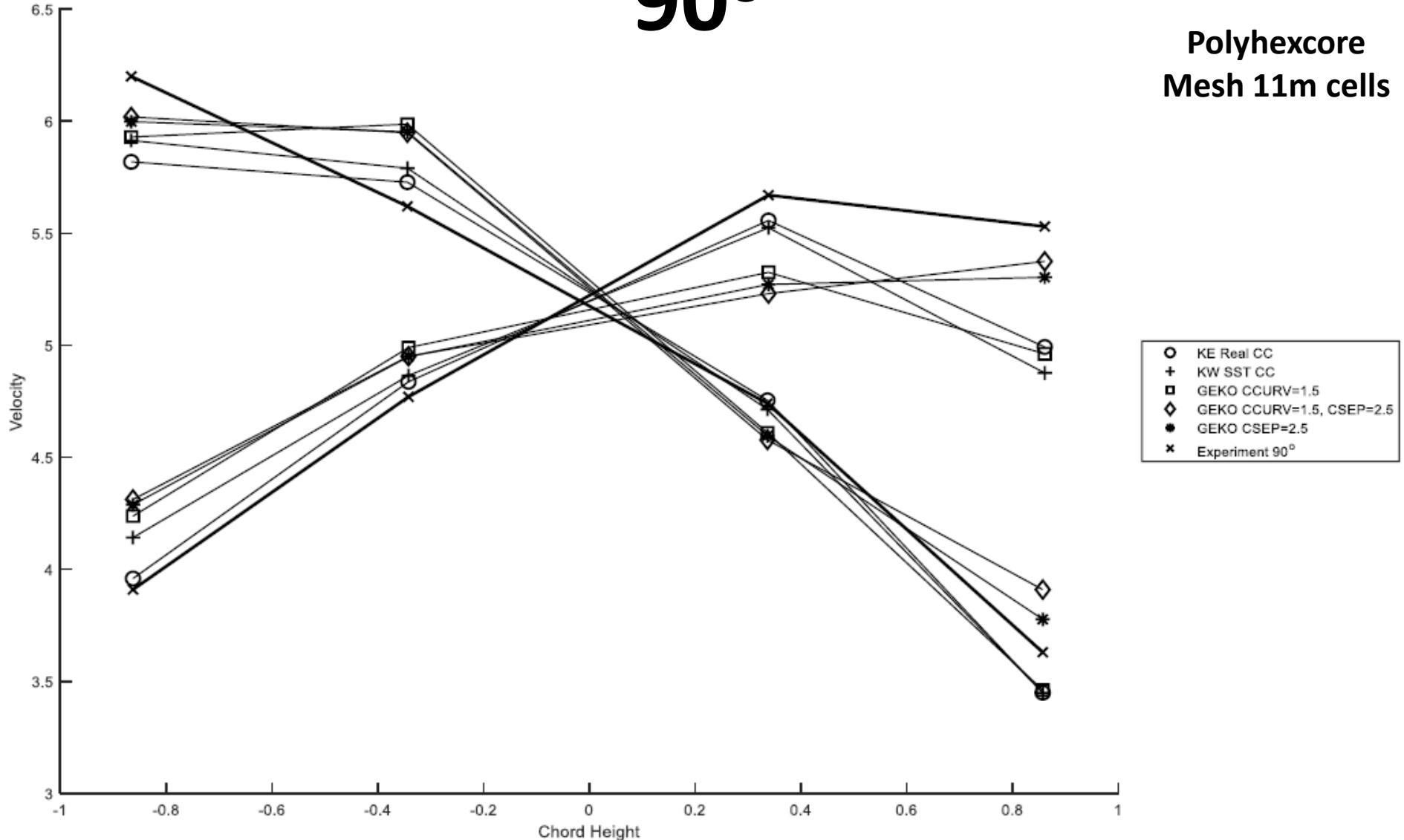
Polyhexcore
Mesh 11m cells



CFD Triple Bend – With Cavities

90°

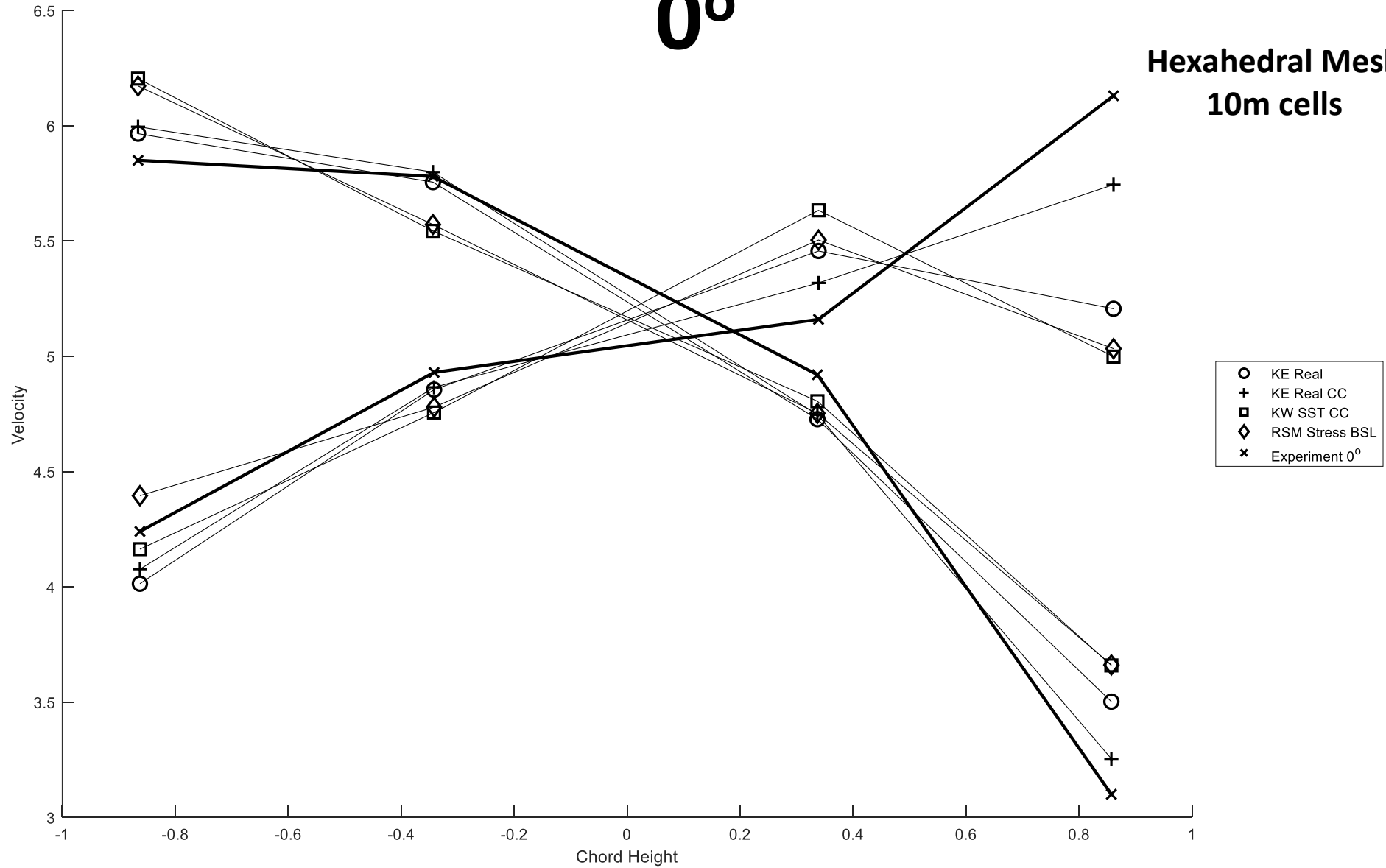
**Polyhexcore
Mesh 11m cells**



CFD Triple Bend – No Cavities

0°

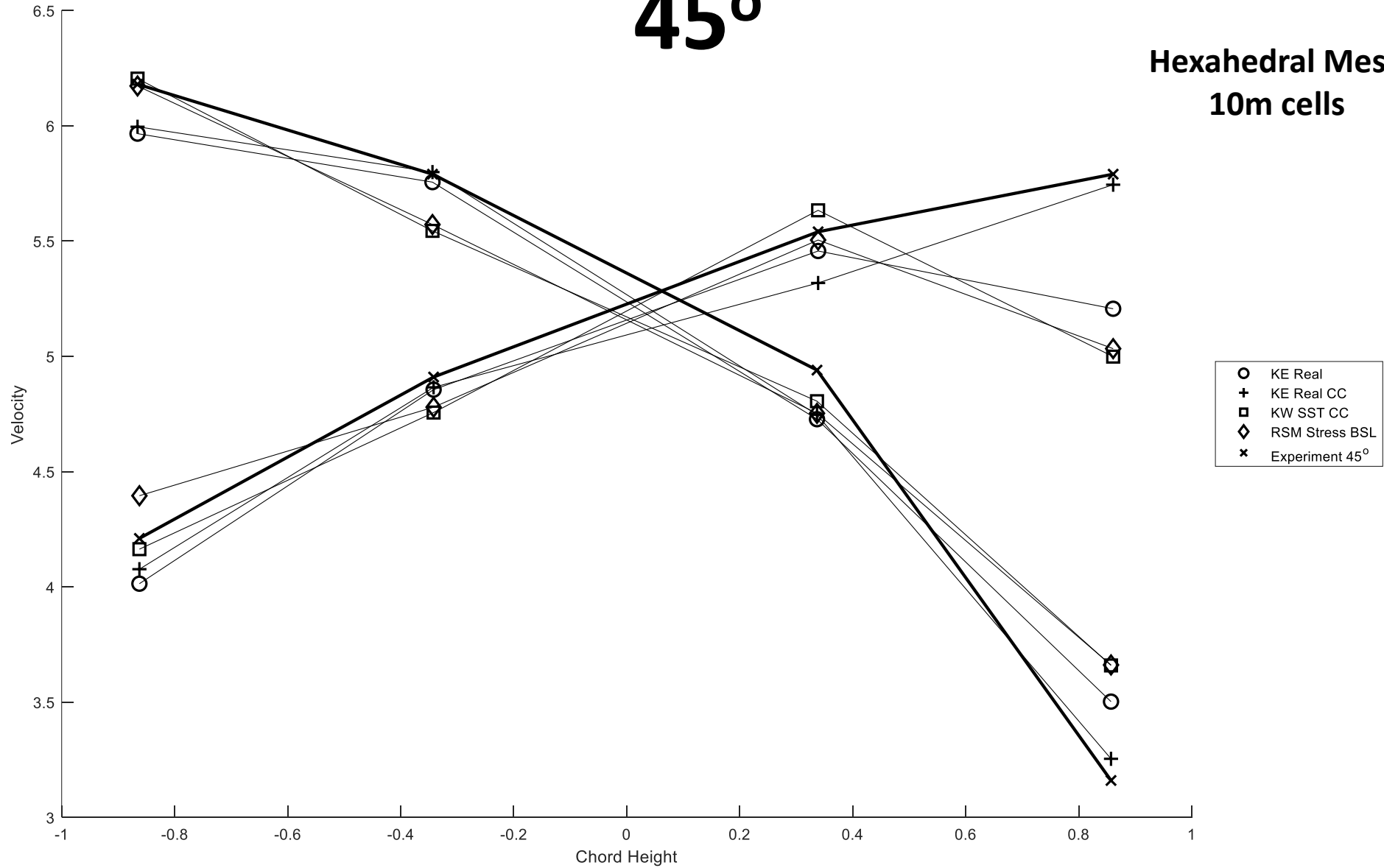
Hexahedral Mesh
10m cells



CFD Triple Bend – No Cavities

45°

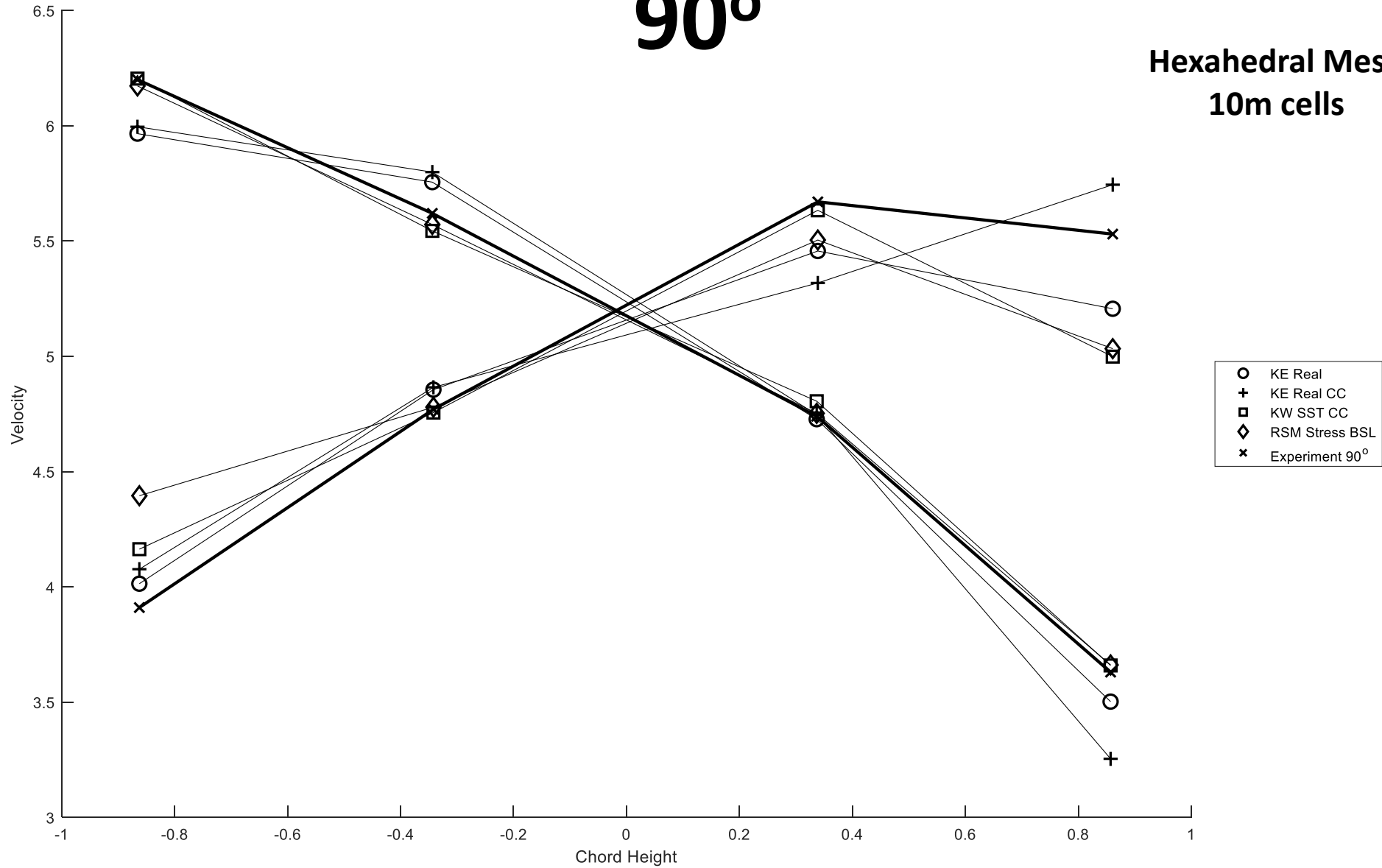
Hexahedral Mesh
10m cells



CFD Triple Bend – No Cavities

90°

Hexahedral Mesh
10m cells



Summary

- Modelling the performance of integration schemes for UFM's of the type and size tested required a detailed CFD model **coupled with an acoustic model** to produce findings consistent with experiment in straight pipe
- The CFD model in this work struggled to model the triple out-of-plane bend which produced a low axial velocity region due to boundary layer separation. This appears partly due to not accurately modelling swirl rotation with findings consistent across turbulence models

